

Ionic Conductance of Carbon Nanotubes: Confronting Literature Data with Nanofluidic Theory

Manoel Manghi,* John Palmeri, François Henn, Adrien Noury, Fabien Picaud, Guillaume Herlem, and Vincent Jourdain*



Cite This: <https://doi.org/10.1021/acs.jpcc.1c08202>



Read Online

ACCESS |



Metrics & More

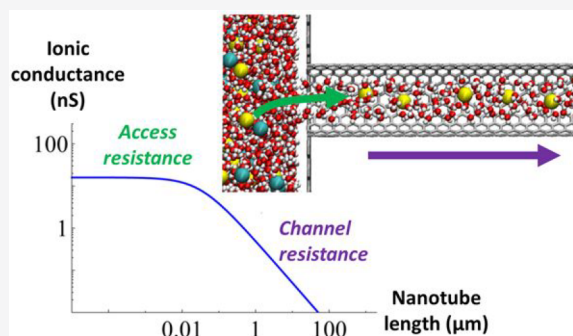


Article Recommendations



Supporting Information

ABSTRACT: The field of ion transport through carbon nanotubes (CNTs) is marked by a large variability of the ionic conductance values reported by different groups. There is also a large uncertainty concerning the relative contributions of channel and access resistances in the experimentally measured currents, both depending on experimental parameters (nanotube length and diameter). In this Perspective, we discuss the ionic conductance values reported so far in the case of individual CNTs and compare them with standard nanofluidic models considering both the access and channel resistances. With a view toward guiding experimentalists, we thus show in which conditions the access or the channel resistance can predominate in CNTs. We explain in particular that it is not justified to use phenomenological models neglecting the channel resistance in the case of micrometer long CNTs. This comparison reveals that most experimental conductance values can be explained in the framework of current nanofluidic models by considering experimental variations of slip length and surface charge density and that just a few extraordinarily high values cannot be accounted for even by using extreme parameter values. Finally, we discuss how to complete existing models and how to improve the statistical reliability of experimental data in the field.



INTRODUCTION

Over the past 20 years, fluid and ion transport through carbon nanotubes (CNTs) has been the subject of intense research revealing a variety of remarkable and exotic behaviors.^{1–3} However, this field of research is still marked by the difficulty in performing reliable experimental measurements, especially at the scale of an individual nanotube, resulting in low measurement statistics and a high variability in conditions and results between different groups. For instance, Amiri et al. reported the highest ionic conductance values to date, all CNT lengths combined, on the order of 70–150 nS at 1 M KCl for a single nanotube 20 μm long.⁴ By comparison, the highest value ever reported by the Bocquet and Siria's group, who studied single CNTs that are both much wider (4–20 nm in diameter) and much shorter (1–3 μm in length), is only 4.5 nS at 1 M KCl.⁵ Even more strikingly, the value measured with high reproducibility by Noy's group for single CNTs with similar diameters (1.5 nm), but 2000 times shorter (10 nm), is only 0.77 nS at 1 M KCl,⁶ which is more than 2 orders of magnitude lower than the values reported in ref 4.

On the theoretical side, there is also controversy on whether ion transport is governed by the access resistance at the nanotube entrance or by the channel resistance associated with the CNT length (Figure 1a). For instance, Amiri et al.⁴ claimed that 20 μm long CNTs with diameters around 1.5 nm were

mimics of biological ion channels (BICs) in that the ion transport properties of these CNTs could be reproduced by using only a simple model of access resistance (i.e., neglecting channel resistance) used for certain types of BICs.⁷ In contrast, most theoretical work to date^{8–10} considered only the channel resistance (inverse conductance), which scales as the channel length L , and neglected the access resistance, which depends on the pore radius but not the pore length, because of the very high aspect ratio of the studied CNTs. The problem is complicated because the ionic conductance of a CNT depends not only on its geometrical features but also on additional parameters, such as the surface charge density at the CNT wall, the fluid slip length at the CNT/water interface, and the type and number of chemical groups at the CNT mouths.

In this Perspective, we will first graphically summarize the ionic conductance values reported to date in the literature for single CNTs. Then, we will discuss in which conditions it is possible to neglect the access or channel resistance of CNTs

Received: September 17, 2021

Revised: October 1, 2021

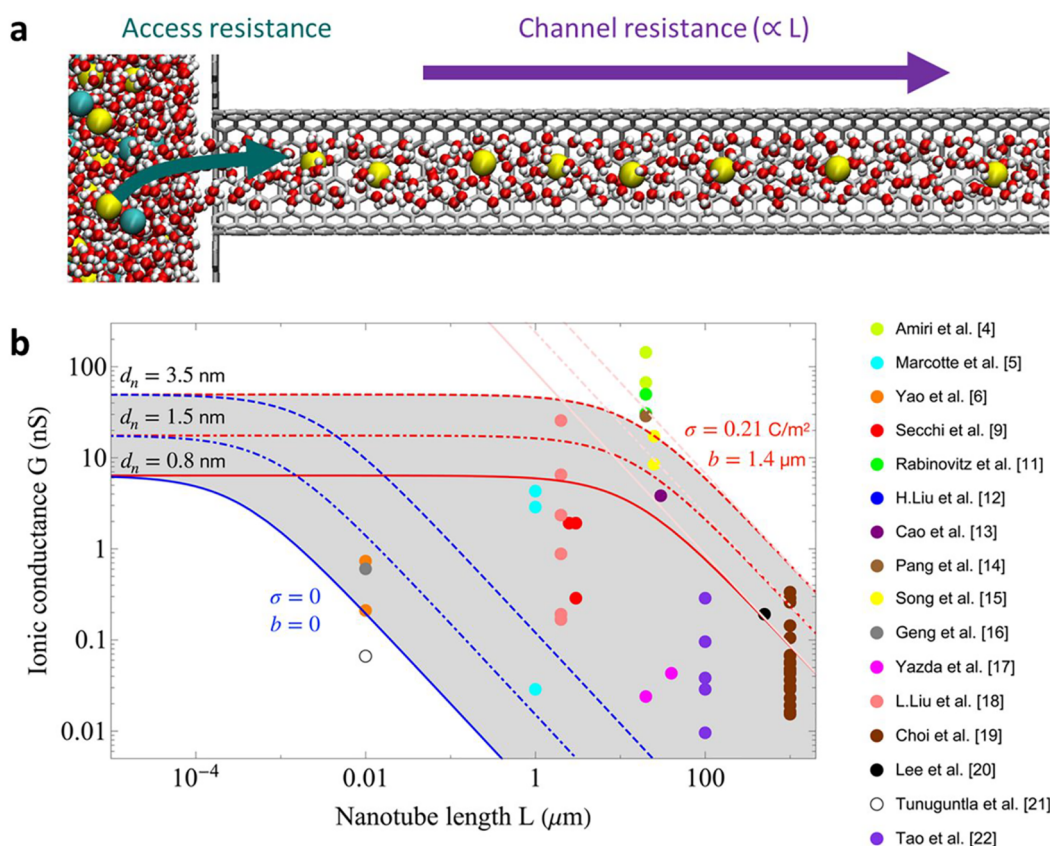


Figure 1. (a) Snapshot from molecular dynamics simulations illustrating the two types of resistance encountered by ions during their transport through carbon nanotubes: access resistance and channel resistance (TIP3P water model, $[\text{NaCl}] = 1 \text{ M}$, surface charge density $= -0.036 \text{ C/m}^2$). (b) Experimental ionic conductance G (in nS) versus the nanopore length L (in μm) reported in the literature (as data points). The curves correspond to the model where the access resistance and the pore resistance are added in series. The radius values are $r = 0.2 \text{ nm}$ (solid line), 0.55 nm (dotted-dashed line), and 1.55 nm (dashed line). The nominal diameter d_n of the CNT is indicated (as explained in the text, a van der Waals distance of 0.2 nm was subtracted from the nominal CNT radius to account for the effective inner radius of the CNT channel). The blue curves correspond to vanishing surface charge density ($\sigma = 0$) and slip length ($b = 0$); the red (pink) curves correspond to eq 2 with $\sigma = 0.21 \text{ C/m}^2$ and $b = 1.4 \mu\text{m}$ with $r_{\text{app}} = r$ (eq 3 with $r_{\text{app}} = r + l_{\text{Du}}/2$). The gray zone corresponds to the region delimited by these two extreme cases for the choice $r_{\text{app}} = r$. For short nanopores G does not depend on L , whereas it decreases as $1/L$ for long nanopores. With the choice $r_{\text{app}} = r + l_{\text{Du}}/2$ this crossover occurs for $L \approx 2\pi r$. The experimental values were taken from Amiri et al.,⁴ Marcotte et al.,⁵ Yao et al.,⁶ Secchi et al.,⁹ Rabinovitz et al.,¹¹ H. Liu et al.,¹² Cao et al.,¹³ Pang et al.,¹⁴ Song et al.,¹⁵ Geng et al.,¹⁶ Yazda et al.,¹⁷ L. Liu et al.,¹⁸ Choi et al.,¹⁹ C. Y. Lee et al.,²⁰ Tunuguntla et al.,²¹ and Tao et al.²²

based on the standard nanofluidic models describing each contribution to the total resistance. We will thus provide theoretical curves combining both access and channel resistances to evidence the lowest and highest theoretically possible values of ionic conductance through CNTs based on the current range of reported parameter values. Finally, we will discuss future developments important for and specific to ion transport in CNTs, in terms of both theoretical modeling and experimental data reliability.

CONFRONTING LITERATURE DATA WITH NANOFLUIDIC THEORY

Figure 1b summarizes the ionic conductance values reported to date in the literature for single CNTs at 1 M KCl (or 3 M if 1 M was not available) and pH close to 7 as a function of the CNT length L (detailed data are given in the Supporting Information). Most measurements were based on the comparison of the ionic conductance of the nanotube devices with that of control devices, while other measurements were based on the current change occurring during stochastic events of nanotube insertion in a membrane or nanotube blockade. From a theoretical perspective, one would expect a plateau at short lengths

corresponding to the access resistance regime and a $1/L$ decrease at long lengths corresponding to the channel resistance regime. In practice, Figure 1b shows a large spread in the experimental data, which may partly be explained by differences in diameters and experimental conditions. Very high values significantly deviating from the theoretically expected trend are particularly observed in the length range of a few tens of micrometers, e.g., ref 4 (light green points) and ref 11 (dark green points).

To account for the literature data, we combined the model of access resistance, G_a^{-1} , generally used in nanofluidics^{23–25} and a model of channel resistance, G_p^{-1} (involving surface charge and slip), commonly used for CNTs.^{8,17,26,27} The total resistance of the nanotube is the sum of these two resistances in series

$$\frac{1}{G} = \frac{1}{G_p} + \frac{1}{G_a}$$

where $G_p = \frac{\pi r^2}{L} \kappa_p$ with L and r the nanopore length and radius, respectively, κ_p the KCl conductivity inside the nanopore, which depends on the uniform surface charge density σ (supposed fixed here), and b the slip length. We have adopted the form for

G_p given in eqs 13 and 14 of ref 26. The access conductance is $G_a = 2r_{\text{app}}\kappa_b$, which is the standard formula obtained by Hall²⁸ when the apparent radius for the access conductance, r_{app} , is set equal to the physical radius r .

This classical model for the access resistance has been generalized, following Lee et al.,²⁹ to the case where spatially extended end effects close to the pore mouth arise in the presence of a nonzero surface charge density σ on the pore wall, which induces a sudden increase of the surface conductivity. The access resistance has the same form as above, but with the radius replaced by an apparent one, $r_{\text{app}} = r + l_{\text{Du}}/2$, where the so-called Dukhin healing length $l_{\text{Du}} = (r/2)(\kappa_s/\kappa_b)$ is proportional to the ratio between the surface conductivity, $\kappa_s = \kappa_p - \kappa_b$, and the bulk one, κ_b . The final conductance, which is probably an upper limit for the influence of entrance effects, is therefore

$$G = \frac{\pi r^2}{L} \frac{\kappa_p}{1 + \frac{\pi r^2 \kappa_p}{2r_{\text{app}} L \kappa_b}} \quad (1)$$

which simplifies, for $r_{\text{app}} = r$, to

$$G = \frac{\pi r^2}{L} \frac{\kappa_p}{1 + \frac{\pi r \kappa_p}{2L \kappa_b}} \quad (2)$$

The crossover between the channel-dominated and access-dominated conductivity would then take place when $L < L_c = \frac{\pi}{2} \frac{\kappa_p}{\kappa_b} r$ and therefore depends on salt concentration and is large for high surface charge densities. In ionic transport models incorporating only electrostatic interactions, $\frac{\kappa_p}{\kappa_b} \geq 1$, and therefore in the $r_{\text{app}} = r$ case, $(\pi/2)r$ is a lower limit (attained at high salt concentration) for the crossover value L_c .

For $r_{\text{app}} = r + \frac{l_{\text{Du}}}{2}$, the expression for G (eq 1) simplifies to

$$G = \frac{\pi r^2}{L} \frac{\kappa_p}{1 + \frac{r}{L} \frac{2\pi}{3\kappa_b/\kappa_p + 1}} \quad (3)$$

This last result has the two following limiting forms:

$$G \approx \frac{\pi r^2}{L} \frac{\kappa_p}{1 + 2\pi \frac{r}{L}} \quad (4)$$

for $\kappa_p \gg \kappa_b$ (low salt concentration/high surface charge density)

and

$$G \approx \frac{\pi r^2}{L} \frac{\kappa_b}{1 + \frac{\pi r}{2L}} \quad (5)$$

for $\kappa_p = \kappa_b$ (high salt concentration/low surface charge density)

Hence, we clearly see that when $r_{\text{app}} = r + \frac{l_{\text{Du}}}{2}$ (eq 3), the effective length $L_c = \frac{2\pi r}{1 + 3\kappa_b/\kappa_p}$, above which the nanopore resistance is larger than the access one and therefore dominates the total conductance, obeys $\frac{\pi}{2}r < L_c < 2\pi r$ and is therefore on the order of r . Even if the adequacy of eq 3²⁹ based on an apparent radius r_{app} remains to be confirmed for different CNT experimental setups, we cite it for completeness and to provide an approximate upper bound. Although this entrance effect might be important for very short nanopores, we conclude that with the choice $r_{\text{app}} = r + l_{\text{Du}}/2$ the total conductance remains

controlled by the nanopore (channel) conductance for nanopores with lengths a few times larger than their radius. For the sake of completeness, we note that two other groups studied the influence of the pore surface charge density on the access resistance. Luchinsky et al.³⁰ computed the total conductance for a very short charged nanopores (BIC) and found numerically a value about 3 times larger than the Hall one at 1 M (see Figure 10 of ref 30). Noh and Aluru³¹ assumed that the conductivity in the bulk in the vicinity of the pore mouth is the same as the pore conductivity κ_p . They proposed a total conductance which is similar to eq 4. However, their value of κ_p is lower than the one we propose here because they took into account electric potential leakage and the breakdown of local electroneutrality in the nanopore near the pore entrances. Note, however, that Noh and Aluru recognized explicitly that their model does not fit experimental data obtained by using CNTs.

Now, with these equations combining both access and channel resistances in hand, we can try to frame the experimental data from the literature. To do so, we considered two extreme cases: (a) zero slip and no surface charge (blue curves in Figure 1b) and (b) slip length and surface charge density both extremely high (red curves for eq 2 and pink curves for eq 3 in Figure 1b). To choose these extreme values, we used the highest values reproducibly reported in the literature (i.e., reported by at least two different groups) for the slip length and the surface charge density of carbon nanotubes: 1.4 μm for the slip length^{27,32} and 0.21 C/m² for the surface charge density.^{8,17} Note that it has been shown using molecular dynamics simulations that the slip length decreases when the surface charge density increases.^{33,34} Indeed, surfaces with a high charge density are more hydrophilic, whereas a high slip length is associated with the hydrophobic nature of the surface. Therefore, combining the most extreme values of b and σ independently reported in the literature ($\sigma = 0.21$ C/m² and $b = 1.4$ μm) constitutes in itself an even more extreme limit. To take into account the various CNT diameters found in experimental literature studies (0.7–4.2 nm), we also plotted each curve considering three different diameters: a small (0.8 nm), an intermediate (1.5 nm), and a large (3.5 nm) diameter. With negligible influence, but for the sake of rigor, we also subtracted in each case a van der Waals distance of 0.2 nm (corresponding to the distance between the water molecules and the CNT wall as observed in MD simulations^{26,35–37}) from this nominal CNT radius. Note that this value of 0.2 nm has been measured with two different force fields for water molecules, namely the TIP3P²⁶ and SPC-E^{36,37} models.

The gray zone in Figure 1b corresponds to the region delimited by these two extreme cases: as clearly visible, the vast majority of experimental data are well framed by the two extreme cases irrespective of the choice made for r_{app} . This supports the idea that the variability of experimental values in the literature can be accounted for by variations of slip length and surface charge density related to device fabrication (e.g., structural defects, adatoms, and grafted chemical groups), the nanotube environment (e.g., charge transfer), and/or the measurement conditions (e.g., pH). The most noticeable exceptions are the too low values of ref 21 (white point) and the too high values of ref 4 (light green points). The low value of ref 21 may be explained by the very small diameter (0.8 nm) of the studied nanotubes: in this diameter range, subcontinuum effects (e.g., dehydration barrier, edge chemical groups, and confined water structure) and/or dielectric exclusion³⁸ may significantly decrease the conductance compared with the

nanofluidic models used for Figure 1b. However, in the case of ref 4 (light green points), it is difficult to explain why these high values cannot be accounted for with standard nanofluidic models, even by using the most extreme estimates for the parameters b and σ .

To account for these high conductance values, the authors of ref 4 used a phenomenological model, initially developed for BICs, considering two vestibules connected by a short narrow charged region. For several reasons, it is ill-advised to use such a model for micrometer long CNTs. First, the geometry is very different since this BIC modeling assumes the charge to be present only at the nanopore constriction and is completely omitted in the long nanopore (thus violating electroneutrality inside the pore). Second, the large charge, extracted *a posteriori* from the model, would have imposed the use of the full Poisson–Boltzmann approach at low salt concentration, i.e., ≤ 0.1 M (see for instance refs 26 and 8), instead of the Debye–Hückel approximation. Third, the pore diameter is fitted from eq 3 of ref 4 where the conductance is assumed to be independent of the nanopore radius, which is unphysical because this quantity clearly depends on the pore radius, as explained above (see eq 1). Fourth and most importantly, the model completely neglects the channel resistance which we argue is the dominant term for micrometer long CNTs when the pore radius is in the nanometer range, as evidenced in Figure 1b for the physically motivated choice $r_{\text{app}} = r + l_{\text{Du}}/2$.

■ FURTHER DEVELOPMENTS IN NANOFUIDIC MODELING

The basic mean-field type transport model adopted here to study the conductance of CNTs incorporates, as is usual in this context, nanopore (electrostatic) surface charge effects and includes contributions from ionic electrical migration, electro-osmosis, and fluid slip. This model does not, however, integrate certain mechanisms that may be important in ionic partitioning into nanopores (and have already been included at least in part in nanofiltration modeling).^{39–41} These additional, generally ion specific, mechanisms go beyond the commonly employed Poisson–Boltzmann mean field theory and include steric exclusion and ion self-energy effects.^{39–44}

To motivate the clear interest in investigating these additional mechanisms involving physical interactions other than the fixed charge electrostatic one (Donnan), we cite the extensive work on specific ion effects:^{45,46} ions of the same charge valency do not in general behave identically in aqueous environments. For example, ions of the same charge do not partition into nanopores and membranes in the same way, although the Donnan (electrostatic) mechanism predicts that they should. It is therefore important to include other physical interactions that depend on the specific ion characteristics (such as size and polarizability) to enhance our understanding of ionic transport through nanopores. One outstanding example is the rejection of halides by nanofiltration membranes:⁴⁷ despite having the same charge the halide anions experience very different rejections. The Donnan (electrostatic) mechanism is clearly not the whole story and predictive modeling can only be reached through a thorough understanding of all the major interactions at play in such systems.

The Born self-energy contribution depends sensitively on ionic charge and radius as well as the dielectric mismatch⁴⁸ between the nanopore-confined electrolyte and the external reservoir (bulk) one.^{39,41,44} The dielectric self-energy depends on ion charge and the dielectric mismatch between the nanopore

confined electrolyte and the surrounding medium constituted by the CNT and its matrix^{39–44} (Figure 2a). Because this

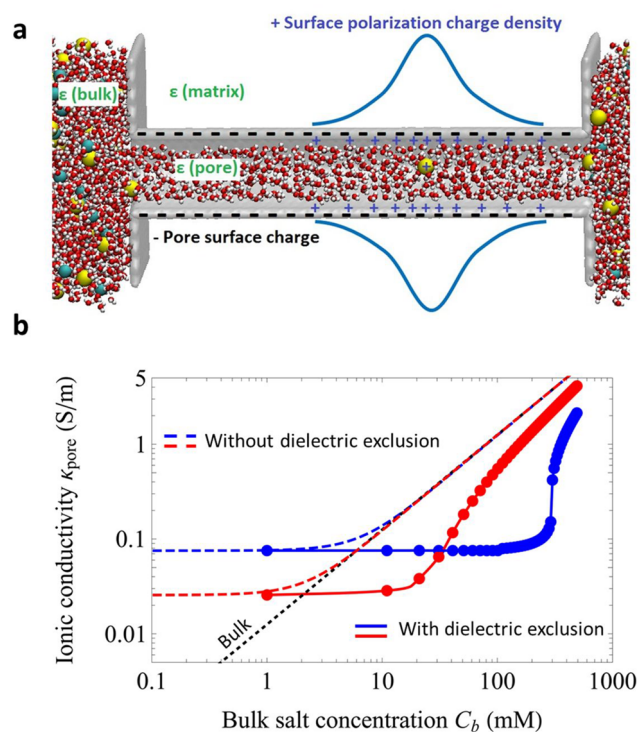


Figure 2. (a) Picture illustrating the effect of the dielectric mismatch between the nanopore confined electrolyte and the medium surrounding the CNT. (b) Comparison of the theoretical conductivity of a slightly charged cylindrical nanopore vs the salt concentration in the reservoirs C_b (blue: $R = 0.7$ nm, $\sigma = 0.5$ mC/m², red: $R = 1.2$ nm, $\sigma = 0.3$ mC/m²) using the mean-field approach (dashed lines, the black dotted line corresponds to the bulk conductivity) and the approach developed in ref 41, which takes into account both hard core volume effects and dielectric exclusion (theoretically computed points, lines are guides for the eye), but not the Born self-energy because we have assumed that the confined and bulk electrolytes have the same dielectric constant. The matrix (or membrane) dielectric constant is $\epsilon(\text{matrix}) = 2$, much lower than the bulk water value $\epsilon(\text{bulk}) = \epsilon(\text{pore}) = 78$ (see part a). Clearly these nonspecific dielectric effects lead to a substantial decrease of the conductivity at intermediate reservoir salt concentrations ($5 < C_b < 500$ mmol/L) to values lower than in the bulk, revealing a faster descent to the low salt concentration (good co-ion exclusion) plateau. This kind of dielectric induced descent could potentially be misinterpreted as being due to surface regulation charge effects, underscoring the subtlety in disentangling the various physical and physicochemical mechanisms at play in ionic transport through nanopores.

external medium usually has low dielectric constant, the dielectric self-energy contribution should be strongly repulsive for tight CNTs. As an example, Figure 2b shows the influence of this type of dielectric mismatch on the theoretical conductivity in slightly charged nanopores: whereas at the mean-field level the dashed curves show the classical behavior of the variation of pore conductance $G(C_b)$ with reservoir salt concentration C_b for a constant surface charge density σ (with a plateau controlled by σ at low C_b and a linear bulk behavior at large C_b , as detailed in refs 8, 9, and 25), the dielectric mismatch induces a lower value at intermediate C_b due to dielectric exclusion.^{40–42} So these effects may potentially be important, and they do have experimentally measurable signatures: it is clear, for example,

from Figure 2b that the nanopore conductivity is always higher than the bulk one if only the Donnan mechanism is taken into account, whereas in the presence of additional dielectric exclusion effects, the nanopore conductivity will be lower than the bulk one at high and intermediate bulk salt concentration and higher at low enough bulk salt concentration (the bulk conductivity is given by the black dotted line). At high enough bulk salt concentration dielectric exclusion dominates even in the presence of pore surface charge. At low enough bulk salt concentration co-ions are excluded from the pore, and the concentration of counterions is determined uniquely by the pore surface charge density to satisfy overall electroneutrality. When dielectric exclusion is present, the bulk salt concentration at which the crossover between these two regimes takes place provides key information about its strength. Furthermore, by studying nanopore conductivity for different salts, such as the halides with a common cation, it should be possible to distinguish between dielectric exclusion, which in its simplest form depends only on the ion valencies, and Born exclusion, which also depends on the ion size.

More generally, the influence on conductance of a spatially varying dielectric constant that arises in the presence of an electrolyte confined in a nanopore needs to be further assessed.⁴⁹ Additional self-energy effects arise from Debye–Hückel type ionic correlations related to differences in ionic solvation between the electrolyte in the pore and in the bulk.^{42–44} Furthermore, the importance of ion pairing³⁹ and ionic polarizability in transport through CNTs needs to be further investigated, especially their role in nanopore conductance. The role and importance of the theoretically predicted ionic “liquid–vapor” phase separation^{42–44} on nanopore conductance remains an open question and very likely requires targeted simulation and experimental studies before clear answers can be provided.

More sophisticated theoretical approaches that would allow access to the confined electrolyte dielectric constant⁴⁹ consist in including explicitly the solvent (water) molecules as self-orienting permanent dipoles.⁵⁰ More work is also needed to clarify the mechanisms of CNT surface charge generation involving ion association and adsorption, especially of H⁺ and OH[−] ions, and the influence of nanopore surface charge and dielectric mismatch on both fluid slip and ionic mobility.⁵¹ We can expect that in the near future the nature of electrolyte transport in CNTs will be further clarified thanks to ongoing work in these areas, a major drive that will surely lead to more successful strategies for optimizing these industrially important nanofluidic devices. One can also hope that substantial progress will be made in the near future in reinforcing the links between all-atom molecular dynamics simulations (both classical and quantum)⁵² and the mesoscopic type theories used here.

IMPROVING THE STATISTICAL RELIABILITY OF EXPERIMENTAL DATA

Even if the variability of the experimental parameters is a likely source of dispersion in the experimental data, it should not distract one from carefully reflecting on the reliability of the experimental data and the way it is statistically evaluated. In general, experimental data obtained with nanotube devices are compared with those obtained with control devices prepared in the same conditions, but without nanotubes (or with closed-end nanotubes). The key question is then, “is there a sufficient statistical difference between nanotube devices and control devices so that one can reliably assign the measured values to ion

transport through the nanotube(s)?” Contrary to other fields, such as the life sciences and most subfields of physics and chemistry, this statistical analysis is often minimal or simply missing in the CNT field, usually because of the difficulty in fabricating a sufficiently large number of both nanotube and control devices. For instance, the total number of measured nanotube and control devices and their responses are often not reported and compared in detail. An alternative reliability assessment could be based on identifying an experimental signature specific to ion transport through CNTs. An empirical criterium quite commonly used is that the ionic conductance G through CNTs should display a power-law dependence with concentration, i.e., $G \approx C^\alpha$, with α close to 1/3. However, non-nanotube systems may display a similar behavior. For instance, Amiri et al. reported data on control devices (i.e., leaky PMMA devices without nanotubes) displaying a power-law dependence with α close to 1/3 (see Figure S5 in ref 4). This 1/3 dependence should therefore not be *a priori* considered as a proof of ion transport through CNTs, unless statistical evidence specific to the studied devices (for both nanotube and control devices) is provided. We strongly believe that a detailed statistical comparison of the responses of nanotube and control devices should now become standard practice for publications in the field.

CONCLUSION

We have provided theoretical curves based on standard nanofluidic theory to help experimentalists to assess (i) in which conditions the access or channel resistance can predominate and (ii) what the highest possible conductance values are based on currently reported physical parameter values. The result that the vast majority of data in the literature can be bounded by using a large but physically reasonable range of slip length and surface charge density values suggests that the experimental variability of these parameters may partly, but not only, account for the diversity of experimental values. We believe that the path toward a better understanding of ion transport through CNTs requires both a better assessment of these parameters and a stronger statistical evaluation of experimental data.

ASSOCIATED CONTENT

Supporting Information

The Supporting Information is available free of charge at <https://pubs.acs.org/doi/10.1021/acs.jpcc.1c08202>.

Tables S1 and S2 detailing ionic conductance values for single or a few CNTs in the literature (PDF)

AUTHOR INFORMATION

Corresponding Authors

Manoel Manghi – *Laboratoire de Physique Théorique, UMR 5152 CNRS-UPS, Université Toulouse III Paul Sabatier, 31062 Toulouse, France*; orcid.org/0000-0002-0146-3950; Email: manghi@irsamc.ups-tlse.fr

Vincent Jourdain – *Laboratoire Charles Coulomb, Univ de Montpellier, CNRS, 34090 Montpellier, France*; orcid.org/0000-0002-2695-078X; Email: vincent.jourdain@umontpellier.fr

Authors

John Palmeri – *Laboratoire Charles Coulomb, Univ de Montpellier, CNRS, 34090 Montpellier, France*

François Henn – *Laboratoire Charles Coulomb, Univ de Montpellier, CNRS, 34090 Montpellier, France*

Adrien Noury – *Laboratoire Charles Coulomb, Univ de Montpellier, CNRS, 34090 Montpellier, France*

Fabien Picaud – *Laboratoire de Nanomédecine Imagerie et Thérapeutique (NIT), EA4662, UFR ST & CHU Médecine, Université de Bourgogne Franche-Comté, 25000 Besançon, France; orcid.org/0000-0002-0570-394X*

Guillaume Herlem – *Laboratoire de Nanomédecine Imagerie et Thérapeutique (NIT), EA4662, UFR ST & CHU Médecine, Université de Bourgogne Franche-Comté, 25000 Besançon, France; orcid.org/0000-0002-9168-7850*

Complete contact information is available at:
<https://pubs.acs.org/10.1021/acs.jpcc.1c08202>

Notes

The authors declare no competing financial interest.

Biographies



Manoel Manghi is Associate Professor at the University Toulouse III - Paul Sabatier (France) since 2005. He is a theoretical physicist working on the statistical physics of soft matter and biophysics. His recent research focus on DNA in single particle experiments and in microfluidics, nanodomains in biomembranes, and nanofluidics of electrolytes. He graduated from the ENS Lyon, obtained his Ph.D. in theoretical physics from the University of Grenoble in 2002, and performed postdoctoral work at the University Ludwig Maximilian of Munich and the University of Montpellier.



John Palmeri is a Senior Research Scientist at the French CNRS currently working at the Laboratoire Charles Coulomb of the CNRS/University of Montpellier. He is a theoretical physicist who focuses on applying the methods of statistical physics to problems in nanofluidics, nanofiltration, biophysics, and soft matter. He obtained a B.A. in physics from Princeton University and a Ph.D. in physics from the

University of Illinois at Urbana–Champaign and performed postdoctoral work at the Institut de Physique Théorique in Saclay (France) and the Institut Laue-Langevin in Grenoble (France).



François Henn is professor at the University of Montpellier where he teaches thermodynamics, electrochemistry, and materials science. His main research topic concerns ion dynamics in solids or at solid/gas–liquid interfaces. He has thus conducted studies in the field of (i) solid electrolytes, (ii) gas adsorption in aluminosilicates such as clays and zeolites, and (iii) more recently the transport of liquid electrolytes in carbon nanotubes. He was educated in physical chemistry and materials sciences at the Universities of Rouen (B.A.) and Montpellier (M.Sc.), obtained a Ph.D. between the Universities of Montpellier and Cambridge, and performed a postdoctoral work at the University of Stanford, USA.



Adrien Noury is a CNRS permanent researcher specialized in nanomaterials. He has received a PhD in physics from University Paris Sud in 2014. He then moved to Barcelona for a postdoctoral stay at ICFO from 2014 to 2017. He has worked experimentally on optics, electronics, and nanomechanics of nanocarbons (e.g., carbon nanotubes and graphene). His current focus is on confinement of matter inside carbon nanotubes, including water and ions. He is also a specialist of microfabrication techniques for devices embedding nanomaterials.



Fabien Picaud is currently director of the Franche-Comté Computing Mesocenter and codirector of the Nanomedicine, Imaging and Therapeutics Laboratory of the University of Burgundy Franche-Comté. His research concerns high performance computing in molecular physics and biophysics. His main topic focuses on the study of the stability of molecular species confined in nanostructures for medical or physical purposes.



Guillaume Herlem is assistant professor in physical chemistry at the University of Franche-Comte since 1998. He graduated from the University of Pierre & Marie Curie in 1994 and obtained his Ph.D. from the University of Franche-Comte in 1997 on liquid electrolyte structures for electrical energy storage. He is now interested in biomaterials for nanomedicine such as biosensors, synthesis of nanovectors, and modification of implantable prostheses by chemistry in mild conditions and modeling of (electro)chemical reactions by DFT.



Vincent Jourdain is a professor in Materials Science at the University of Montpellier, France. His main interests are the physics and chemistry of carbon nanostructures, especially including their growth mechanisms,

their nanofluidic properties, and their optical characterization. His approach notably involves *in situ* measurements by Raman spectroscopy, optical polarization microscopy, microfabrication, and low-noise electrical measurements. He obtained a Ph.D. in Materials Science from the University of Montpellier (France) in 2003 and performed postdoctoral work at the Engineering Department of the University of Cambridge (UK) from 2004 to 2005. He was a member of the Institut Universitaire de France from 2015 to 2020.

ACKNOWLEDGMENTS

The authors acknowledge the support of the Agence Nationale de la Recherche (ANR-18-CE09-0011-01 "IONESCO"). V.J. acknowledges the support of the Institut Universitaire de France (IUF). A.N. acknowledges the support of the CNRS-MITI through a "Momentum" grant.

REFERENCES

- (1) Majumder, M.; Siria, A.; Bocquet, L. Flows in One-Dimensional and Two-Dimensional Carbon Nanochannels: Fast and Curious. *MRS Bull.* **2017**, *42* (4), 278–282.
- (2) Faucher, S.; Aluru, N.; Bazant, M. Z.; Blankschtein, D.; Brozena, A. H.; Cumings, J.; Pedro de Souza, J.; Elimelech, M.; Epsztein, R.; Fourkas, J. T.; et al. Critical Knowledge Gaps in Mass Transport through Single-Digit Nanopores: A Review and Perspective. *J. Phys. Chem. C* **2019**, *123* (35), 21309–21326.
- (3) Thiruraman, J. P.; Masih Das, P.; Drndić, M. Ions and Water Dancing through Atom-Scale Holes: A Perspective toward "Size Zero". *ACS Nano* **2020**, *14* (4), 3736–3746.
- (4) Amiri, H.; Shepard, K. L.; Nuckolls, C.; Hernández Sánchez, R. Single-Walled Carbon Nanotubes: Mimics of Biological Ion Channels. *Nano Lett.* **2017**, *17* (2), 1204–1211.
- (5) Marcotte, A.; Mouterde, T.; Niguès, A.; Siria, A.; Bocquet, L. Mechanically Activated Ionic Transport across Single-Digit Carbon Nanotubes. *Nat. Mater.* **2020**, *19* (10), 1057–1061.
- (6) Yao, Y.-C.; Taqieddin, A.; Alibakhshi, M. A.; Wanunu, M.; Aluru, N. R.; Noy, A. Strong Electroosmotic Coupling Dominates Ion Conductance of 1.5 Nm Diameter Carbon Nanotube Porins. *ACS Nano* **2019**, *13* (11), 12851–12859.
- (7) Nelson, A. P.; McQuarrie, D. A. The Effect of Discrete Charges on the Electrical Properties of a Membrane. I. *J. Theor. Biol.* **1975**, *55* (1), 13–27.
- (8) Biesheuvel, P. M.; Bazant, M. Z. Analysis of Ionic Conductance of Carbon Nanotubes. *Phys. Rev. E: Stat. Phys., Plasmas, Fluids, Relat. Interdiscip. Top.* **2016**, *94* (5), 50601.
- (9) Secchi, E.; Nigues, A.; Jubin, L.; Siria, A.; Bocquet, L. Scaling Behavior for Ionic Transport and Its Fluctuations in Individual Carbon Nanotubes. *Phys. Rev. Lett.* **2016**, *116*, 154501.
- (10) Manghi, M.; Palmeri, J.; Yazda, K.; Henn, F.; Jourdain, V. Role of Charge Regulation and Flow Slip in the Ionic Conductance of Nanopores: An Analytical Approach. *Phys. Rev. E: Stat. Phys., Plasmas, Fluids, Relat. Interdiscip. Top.* **2018**, *98* (1), 012605.
- (11) Rabinowitz, J.; Cohen, C.; Shepard, K. L. An Electrically Actuated, Carbon-Nanotube-Based Biomimetic Ion Pump. *Nano Lett.* **2020**, *20* (2), 1148–1153.
- (12) Liu, H. T.; He, J.; Tang, J. Y.; Liu, H.; Pang, P.; Cao, D.; Krstic, P.; Joseph, S.; Lindsay, S.; Nuckolls, C. Translocation of Single-Stranded DNA Through Single-Walled Carbon Nanotubes. *Science* **2010**, *327* (5961), 64–67.
- (13) Cao, D.; Pang, P.; Liu, H.; He, J.; Lindsay, S. M. Electronic Sensitivity of a Single-Walled Carbon Nanotube to Internal Electrolyte Composition. *Nanotechnology* **2012**, *23* (8), 085203.
- (14) Pang, P.; He, J.; Park, J. H.; Krstic, P. S.; Lindsay, S. Origin of Giant Ionic Currents in Carbon Nanotube Channels. *ACS Nano* **2011**, *5* (9), 7277–7283.
- (15) Song, W. S.; Pang, P.; He, J.; Lindsay, S. Optical and Electrical Detection of Single-Molecule Translocation through Carbon Nanotubes. *ACS Nano* **2013**, *7* (1), 689–694.

- (16) Geng, J.; Kim, K.; Zhang, J.; Escalada, A.; Tunuguntla, R.; Comolli, L. R.; Allen, F. I.; Shnyrova, A. V.; Cho, K. R.; Munoz, D.; Wang, Y. M.; Grigoropoulos, C. P.; Ajo-Franklin, C. M.; Frolov, V. A.; Noy, A. Stochastic Transport through Carbon Nanotubes in Lipid Bilayers and Live Cell Membranes. *Nature* **2014**, *514* (7524), 612–615.
- (17) Yazda, K.; Tahir, S.; Michel, T.; Loubet, B.; Manghi, M.; Bentin, J.; Picaud, F.; Palmeri, J.; Henn, F.; Jourdain, V. Voltage-Activated Transport of Ions through Single-Walled Carbon Nanotubes. *Nanoscale* **2017**, *9* (33), 11976–11986.
- (18) Liu, L.; Yang, C.; Zhao, K.; Li, J.; Wu, H.-C. Ultrashort Single-Walled Carbon Nanotubes in a Lipid Bilayer as a New Nanopore Sensor. *Nat. Commun.* **2013**, *4*, 2989.
- (19) Choi, W.; Ulissi, Z. W.; Shimizu, S. F. E.; Bellisario, D. O.; Ellison, M. D.; Strano, M. S. Diameter-Dependent Ion Transport through the Interior of Isolated Single-Walled Carbon Nanotubes. *Nat. Commun.* **2013**, *4*, 2397.
- (20) Lee, C. Y.; Choi, W.; Han, J. H.; Strano, M. S. Coherence Resonance in a Single-Walled Carbon Nanotube Ion Channel. *Science* **2010**, *329* (5997), 1320.
- (21) Tunuguntla, R. H.; Henley, R. Y.; Yao, Y.-C.; Pham, T. A.; Wanunu, M.; Noy, A. Enhanced Water Permeability and Tunable Ion Selectivity in Subnanometer Carbon Nanotube Porins. *Science* **2017**, *357* (6353), 792–796.
- (22) Tao, R.; Gao, X.; Lin, D.; Chen, Y.; Jin, Y.; Chen, X.; Yao, S.; Huang, P.; Zhang, J.; Li, Z. The Role of Entrance Functionalization in Carbon Nanotube-Based Nanofluidic Systems: An Intrinsic Challenge. *Phys. Fluids* **2021**, *33* (1), 12015.
- (23) Gravelle, S.; Joly, L.; Ybert, C.; Bocquet, L. Large Permeabilities of Hourglass Nanopores: From Hydrodynamics to Single File Transport. *J. Chem. Phys.* **2014**, *141* (18), 18CS26.
- (24) Rankin, D. J.; Huang, D. M. The Effect of Hydrodynamic Slip on Membrane-Based Salinity-Gradient-Driven Energy Harvesting. *Langmuir* **2016**, *32* (14), 3420–3432.
- (25) Happel, J.; Brenner, H. *Low Reynolds Number Hydrodynamics: With Special Applications to Particulate Media*; Springer Science & Business Media: 2012; Vol. 1.
- (26) Balme, S.; Picaud, F.; Manghi, M.; Palmeri, J.; Bechelany, M.; Cabello-Aguilar, S.; Abou-Chaaya, A.; Miele, P.; Balanzat, E.; Janot, J. M. Ionic Transport through Sub-10 Nm Diameter Hydrophobic High-Aspect Ratio Nanopores: Experiment, Theory and Simulation. *Sci. Rep.* **2015**, *5*, 10135.
- (27) Secchi, E.; Marbach, S.; Niguès, A.; Stein, D.; Siria, A.; Bocquet, L. Massive Radius-Dependent Flow Slippage in Single Carbon Nanotubes. *Nature* **2016**, *537*, 210–213.
- (28) Hall, J. E. Access Resistance of a Small Circular Pore. *J. Gen. Physiol.* **1975**, *66* (4), 531–532.
- (29) Lee, C.; Joly, L.; Siria, A.; Biance, A.-L.; Fulcrand, R.; Bocquet, L. Large Apparent Electric Size of Solid-State Nanopores Due to Spatially Extended Surface Conduction. *Nano Lett.* **2012**, *12* (8), 4037–4044.
- (30) Luchinsky, D. G.; Tindjong, R.; Kaufman, I.; McClintock, P. V. E.; Eisenberg, R. S. Self-Consistent Analytic Solution for the Current and the Access Resistance in Open Ion Channels. *Phys. Rev. E* **2009**, *80* (2), 21925.
- (31) Noh, Y.; Aluru, N. R. Ion Transport in Electrically Imperfect Nanopores. *ACS Nano* **2020**, *14* (8), 10518–10526.
- (32) Holt, J. K.; Park, H. G.; Wang, Y. M.; Stadermann, M.; Artyukhin, A. B.; Grigoropoulos, C. P.; Noy, A.; Bakajin, O. Fast Mass Transport through Sub-2-Nanometer Carbon Nanotubes. *Science* **2006**, *312* (5776), 1034–1037.
- (33) Huang, D. M.; Cottin-Bizonne, C.; Ybert, C.; Bocquet, L. Aqueous Electrolytes near Hydrophobic Surfaces: Dynamic Effects of Ion Specificity and Hydrodynamic Slip. *Langmuir* **2008**, *24* (4), 1442–1450.
- (34) Xie, Y.; Fu, L.; Niehaus, T.; Joly, L. Liquid-Solid Slip on Charged Walls: The Dramatic Impact of Charge Distribution. *Phys. Rev. Lett.* **2020**, *125* (1), 14501.
- (35) Longhurst, M. J.; Quirke, N. The Environmental Effect on the Radial Breathing Mode of Carbon Nanotubes in Water. *J. Chem. Phys.* **2006**, *124* (23), 234708.
- (36) Longhurst, M. J.; Quirke, N. The Environmental Effect on the Radial Breathing Mode of Carbon Nanotubes. II. Shell Model Approximation for Internally and Externally Adsorbed Fluids. *J. Chem. Phys.* **2006**, *125* (18), 184705.
- (37) Pascal, T. A.; Goddard, W. A.; Jung, Y. Entropy and the Driving Force for the Filling of Carbon Nanotubes with Water. *Proc. Natl. Acad. Sci. U. S. A.* **2011**, *108* (29), 11794–11798.
- (38) Neklyudov, V.; Freger, V. Water and Ion Transfer to Narrow Carbon Nanotubes: Roles of Exterior and Interior. *J. Phys. Chem. Lett.* **2021**, *12* (1), 185–190.
- (39) Freger, V. Selectivity and Polarization in Water Channel Membranes: Lessons Learned from Polymeric Membranes and CNTs. *Faraday Discuss.* **2018**, *209*, 371–388.
- (40) Yaroshchuk, A. E. Dielectric Exclusion of Ions from Membranes. *Adv. Colloid Interface Sci.* **2000**, *85* (2–3), 193–230.
- (41) Lanteri, Y.; Fievet, P.; Szymczyk, A. Evaluation of the Steric, Electric, and Dielectric Exclusion Model on the Basis of Salt Rejection Rate and Membrane Potential Measurements. *J. Colloid Interface Sci.* **2009**, *331* (1), 148–155.
- (42) Buyukdagli, S.; Manghi, M.; Palmeri, J. Ionic Exclusion Phase Transition in Neutral and Weakly Charged Cylindrical Nanopores. *J. Chem. Phys.* **2011**, *134* (7), 74706.
- (43) Loubet, B.; Manghi, M.; Palmeri, J. A Variational Approach to the Liquid-Vapor Phase Transition for Hardcore Ions in the Bulk and in Nanopores. *J. Chem. Phys.* **2016**, *145* (4), 44107.
- (44) Hennequin, T.; Manghi, M.; Palmeri, J. Competition between Born Solvation, Dielectric Exclusion, and Coulomb Attraction in Spherical Nanopores. *Phys. Rev. E: Stat. Phys., Plasmas, Fluids, Relat. Interdiscip. Top.* **2021**, *104*, 044601.
- (45) Kunz, W. *Specific Ion Effects*; World Scientific: 2010.
- (46) *Ion Specific Hofmeister Effects*; Faraday Discussions; The Royal Society of Chemistry: 2013.
- (47) Diawara, C. K.; Lô, S. M.; Rumeau, M.; Pontie, M.; Sarr, O. A Phenomenological Mass Transfer Approach in Nanofiltration of Halide Ions for a Selective Defluorination of Brackish Drinking Water. *J. Membr. Sci.* **2003**, *219* (1–2), 103–112.
- (48) Fumagalli, L.; Esfandiari, A.; Fabregas, R.; Hu, S.; Ares, P.; Janardanan, A.; Yang, Q.; Radha, B.; Taniguchi, T.; Watanabe, K.; Gomila, G.; Novoselov, K. S.; Geim, A. K. Anomalous Low Dielectric Constant of Confined Water. *Science* **2018**, *360* (6395), 1339–1342.
- (49) Bonthuis, D. J.; Gekle, S.; Netz, R. R. Profile of the Static Permittivity Tensor of Water at Interfaces: Consequences for Capacitance, Hydration Interaction and Ion Adsorption. *Langmuir* **2012**, *28* (20), 7679–7694.
- (50) Adar, R. M.; Markovich, T.; Levy, A.; Orland, H.; Andelman, D. Dielectric Constant of Ionic Solutions: Combined Effects of Correlations and Excluded Volume. *J. Chem. Phys.* **2018**, *149* (5), 54504.
- (51) Antila, H. S.; Luijten, E. Dielectric Modulation of Ion Transport near Interfaces. *Phys. Rev. Lett.* **2018**, *120* (13), 135501.
- (52) Chen, X. Molecular Dynamics Simulation of Nanofluidics. *Rev. Chem. Eng.* **2018**, *34* (6), 875–885.